Irradiation of the photoisomer of V (Vc) with ultraviolet light leads to the production of V, and, as with ANPC and IIIc, part of the product is fluorescent, the emission being identical with the exciplex fluorescence obtained by excitation of V. The quantum yield of this electronically excited product is about 10% of the corresponding value observed from irradiation of ANPC at about 100 K in glassy solvents.[11]

Registry No. I, 84599-77-9; II, 94957-24-1; III, 94957-25-2; IIIc, 94957-27-4; IV, 94957-26-3; V, 94978-15-1; DAP, 63934-10-1; HCl, 7647-01-0; 1-(9-anthroyl)-2-(9-anthryl)ethane, 84599-75-7; anthracene, 120-12-7; paraformaldehyde, 30525-89-4; [2.3](9,10)-anthracenophane, 70057-86-2.

Photophysical Studies on 1-(*p*-Aminophenyl)pyrene. Characterization of an Intramolecular Charge-Transfer State with Application to Proton-Transfer Dynamics

Sair Hagopian and Lawrence A. Singer*

Contribution from the Department of Chemistry, University of Southern California, Los Angeles, California 90089-1062. *Received August 29, 1984*

Abstract: A photophysical study on 1-(*p*-aminophenyl)pyrene (I) reveals two principal fluorescences arising from π,π^* (locally excited in pyrene ring) and charge-transfer (CT) (aniline as donor, pyrene as acceptor) states. The latter dominates in organic solvents and aqueous media at pH $\geq$7. The estimated energy of the CT state in highly polar solvents (near 500 nm, $\sim$2.5 eV) agrees well with the measured redox energetics (2.7 eV) while the dependence of the transition energy on solvent dielectric constant indicates an excited state dipole moment of $\sim$14 D. The photophysics of I is pH dependent in aqueous media because of a conjugate acid/base equilibrium with ground- and excited-state constants of pK_a = 4.05, pK_a^* = 3.3 (Forster cycle), respectively, in ethanol-water (50:50). The rather similar acidities of the ground and excited states of I indicate little or no CT contribution to the deprotonation step in the excited state. Deprotonation of the locally excited π,π^* state of I (conjugate acid form) is thought to initially yield the locally excited free base form of I which rapidly relaxes to the CT state. The latter is subject to proton-transfer quenching (most likely involving the pyrene radical anion moiety of the CT state), k_q = (7.38 $\pm$ 1.5) $\times$ 10^8 M^{-1} s^{-1} (corrected for changing proton activity coefficients in ethanol-water). A study of the rate of deprotonation of the conjugate acid of I* from room temperature through the liquid/solid phase transition (near $\sim$50 °C) to -196 °C allows an estimate of the enthalpy and entropy of activation in several different regions. As the temperature is lowered from 295 to 160 K, the enthalpy term decreases from 5360 to 780 cal/mol while the entropy term changes from -6.1 to -24.3 cal/(K·mol).

Charge-transfer (CT) interaction is an important contributor to the electronic excited states of molecules.[1] The almost ubiquitous nature of CT in photochemistry arises from the relatively favorable energetics of redox reactions when one of the reactants is photoexcited. Both inter-[2] and intramolecular[3] excited-state CT complexes are known with varying degrees of CT character. One common structural arrangement of these complexes has the interacting π-systems in parallel planes 3 or 4 Å apart.[4] Recently, another type of CT complex has been identified in systems where π-electron donor and acceptor groups, directly connected by a single bond, reside in mutually orthogonal planes. These complexes have been named twisted intramolecular charge-transfer (TICT) complexes.[5] Examples of compounds forming excited-state TICT complexes are *p*-(dimethylamino)benzonitrile[6] (the classical case) and *p*-(9-anthryl)-*N*,*N*-dimethylaniline and derivatives.[7] Dual fluorescences are often observed from these systems arising from a locally excited π,π^* state (which is rather solvent independent) and the TICT state (which is very solvent dependent because of a large dipole moment).

This paper describes the photophysics of 1-(*p*-aminophenyl)-pyrene (I),[8] which is dominated by a low-energy TICT state. The dual fluorescences observed in this system, which arise from locally excited, π,π^* (conjugate acid) and TICT (free base) states, may be readily modulated by pH. An important observation is the apparent uncoupling of deprotonation of the locally excited conjugate acid from transformation of the π,π^* into the TICT state. Finally, we demonstrate the usefulness of I as a probe of proton-transfer dynamics over a wide temperature range.

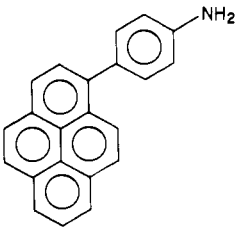

I

Results and Discussion

Synthesis and Structure of 1-(*p*-Aminophenyl)pyrene. Compound I was synthesized by conventional procedures starting with coupling of *p*-nitrophenyldiazonium chloride with pyrene. Careful column chromatography led to isolation of both 1-(*p*-nitrophenyl)- and 2-(*p*-nitrophenyl)pyrene. Both compounds were reduced to the corresponding amines (Sn/HCl). Mass spectral analysis confirmed the formulas of both the nitro and amino compounds while the structures of the 1- and 2-isomers were elucidated by

(1) Beens, H.; Weller, A. In "Organic Molecular Photophysics"; Birks, J. B.; Ed.; Wiley: New York, 1975; Vol 2, and references therein.
(2) (a) Leonhardt, H.; Weller, A. *Ber. Bunsenges. Phys. Chem.* **1963**, *67*, 791. (b) Ottolenghi, M. *Acc. Chem. Res.* **1973**, *6*, 153 and references therein. (c) Mataga, N.; Ottolenghi, M. In "Molecular Association"; Foster, R., Ed.; Academic Press: London, 1979; Vol. 2.
(3) (a) Chandross, E. A.; Thomas, H. T. *Chem. Phys. Lett.* **1971**, *9*, 393. (b) Ide, R.; Sakata, Y.; Misumi, S.; Okada, T.; Mataga, N. *J. Chem. Soc. Chem. Commun.* **1972**, 1009. (c) Okado, T.; Kuyjito, K.; Kubota, M.; Mataga, N.; *Chem. Phys. Lett.* **1973**, *24*, 563. (d) Van der Auweraer, M.; Gilbert, A.; De Schryver, F. C. *J. Am. Chem. Soc.* **1980**, *102*, 4007 and references therein.
(4) (a) Hirayama, F. *J. Chem. Phys.* **1965**, *42*, 3163. (b) Mimura, T.; Itoh, M. *J. Am. Chem. Soc.* **1976**, *98*, 1095.
(5) Siemiarczuk, A.; Koput, J.; Pohorille, A. *Z. Naturforsch., A* **1982**, *37A*, 598 and references therein.
(6) (a) Rotkiewicz, K.; Grellmann, K. H.; Grabowski, Z. R. *Chem. Phys. Lett.* **1973**, *19*, 315. (b) Rotkiewicz, K.; Grabowski, Z. R.; Krowczynski, A. *J. Lumin.* **1976**, *12/13*, 877.
(7) Siemiarczuk, A.; Grabowski, Z. R.; Krowczynski, A.; Ascher, M.; Ottolenghi, M. *Chem. Phys. Lett.* **1977**, *51*, 315.
(8) For a preliminary account of some aspects of this work see: Hagopian, S.; Singer, L. A. *J. Am. Chem. Soc.* **1983**, *105*, 6760.

0002-7863/85/1507-1874$01.50/0

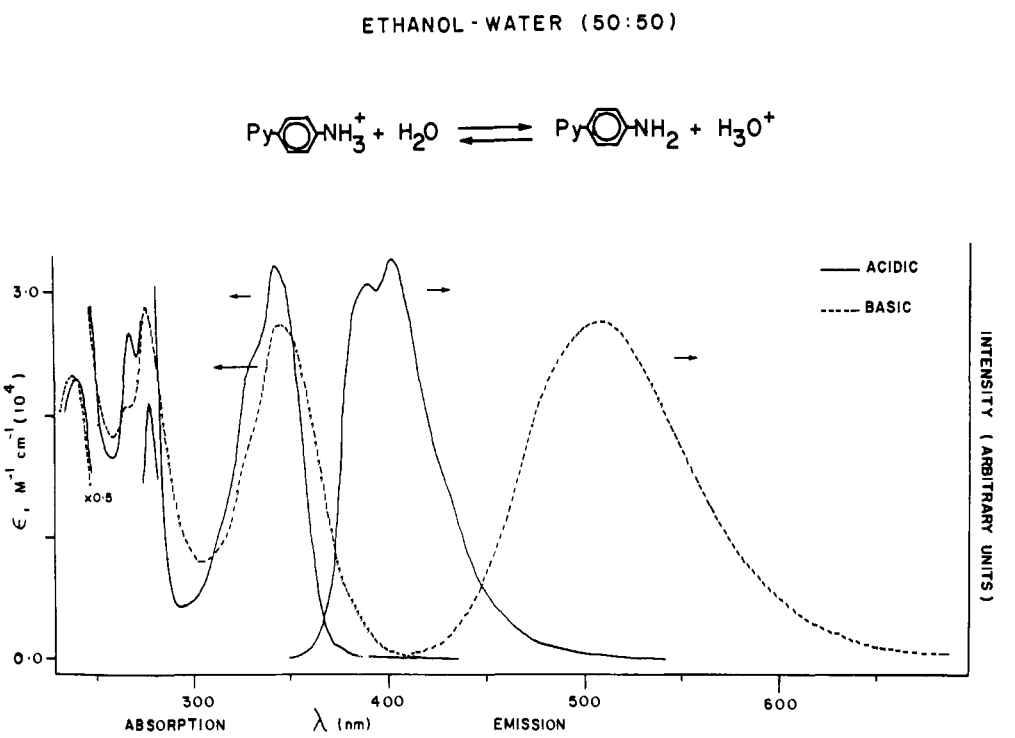

Figure 1. Absorption and emission spectra of conjugate acid and base forms of 1-(*p*-aminophenyl)pyrene in ethanol–water (50:50).

FT ^{13}C NMR spectroscopy. This paper describes results obtained with the 1-isomer. Preliminary studies on 2-(*p*-aminophenyl)-pyrene indicate the presence of a low-lying CT state in this system as well, but detailed results have not as yet been obtained.

Several structural features in I are noteworthy. The stereochemistry of the *p*-aminophenyl group in the 1-position of the pyrene ring is identical with that in 1-phenylnaphthelene. Because of severe H–H repulsions, the energy minima for the ground and S_1 states in the latter occur at twist angles (phenyl relative to naphthalene) of 50° and 32°, respectively, according to recent calculations.[9] We assume that similar skewed geometries apply to I and are incorporated into the potential energy diagram described below.

Ground-State Acidity and Cyclic Voltammogram Measurements. The ground-state pK_a of I was measured to be 4.05 by potentiometric titration in ethanol–water (50:50) which is a typical value for an aniline.[10] A cyclic voltammogram of I in ethanol–water (55:45) with 0.1 M tetrabutylammonium perchlorate as supporting electrolyte indicates two irreversible oxidation waves at 0.67 and 1.2 V vs. Ag/AgCl (0.87 and 1.4 V vs. NHE). The smaller potential, assigned to the oxidation of the aniline ring, is in reasonable agreement with a calculated value of $E_{ox} = 0.9$ (vs. NHE) for aniline in water at pH = 7.[11] Thus, there appears to be little electronic interaction between the pyrene and aniline moieties (as also indicated by the electronic absorption spectra described below) presumably because of the skewed ground-state geometry. The larger oxidation potential may be associated with the pyrene ring in I or in a subsequently formed product since, under the above conditions in ethanol–water (65:35), we measure E_{ox} for pyrene as 1.01 V vs. Ag/AgCl (1.21 V vs. NHE).[13] No reduction wave was observed with I out to ~1.5 V vs. Ag/AgCl which is not unexpected since E_{red} for pyrene in dimethylformamide is ~1.80 V (vs. NHE).[14] These observations predict the availability of an intramolecular CT state in I (aniline as D, pyrene as A) near 2.7 eV in polar media by the relationship

$$E_{ct} = E_{ox}(D^+/D) - E_{red}(A/A^-) - C \qquad (1)$$

where $C = e^2/\epsilon R$ and represents the Coulombic energy gained when two radical ions are brought within an interaction distance R in a solvent of dielectric ϵ. C tends to be small relative to the other parameters in polar media[15] and is usually neglected in estimating E_{ct}.[16]

Table I. Fluorescence Maxima in Solvents of Different Polarity

solvent	dielectric constant	maximum, nm
methylcyclohexane	2.02	407
benzene	2.28	425
ethyl ether	4.34	444
tetrahydrofuran	7.58	466
dichloromethane	8.93	451
n-pentanol	13.9	483
ethanol	24.5	486
benzonitrile	25.2	480
acetonitrile	37.5	490
glycerol	42.5	498
ethanol–water (50:50)	46.0	506
ethanol–water (50:50) at pH 1		400

Electronic Absorption Spectra. The electronic absorption spectrum of I in either polar or nonpolar solvents is almost a simple

(9) Gustav, K.; Kempka, U.; Suhnel, J. *Chem. Phys. Lett.* **1980**, *71*, 280.

(10) Perrin, D. D. "Dissociation Constants of Organic Bases in Aqueous Soluton"; Butterworths: London, 1965.

(11) Bacon, J.; Adams, R. N. *J. Am. Chem. Soc.* **1968**, *90*, 6596. E_{ox} = 1.20 V (vs NHE) at pH 2.3 in water. From the Nernst equation for the oxidation half-reaction for aniline (An), $E = E° (RT/nF) \ln (Q)$, where $Q = [An]/[An^+]$, and from $[An] = k_a[AnH^+]/[H_3O^+]$, it follows that at 25 °C, $E_{ox} = E° + 0.059(pK - pH) - (0.059 \log ([AnH^+]/[An^+]$. In cyclic voltammetry, the characteristic potential at $0.85i_p$ corresponds to $E°$ for a reversible wave.[12] If this approximation holds for the irreversible aniline wave, then the characteristic potential at pH 2.3 corresponds to $E_{ox} \simeq E° + 0.059(pK_a - pH)$ and $E° = 1.06$ V using $pK = 4.6$. In turn, at pH 7, $E_{ox} \simeq 0.90$ V.

(12) Fry, A. J. "Synthetic Organic Electrochemistry"; Harper and Row: New York, 1972; p 82.

(13) This value may be compared with $E_{ox} = 1.40$ V in acetonitrile. Pysh, E. S.; Yang, N. C. *J. Am. Chem. Soc.* **1963**, *85*, 2124.

(14) Given, P. H.; Peover, M. E. *J. Chem. Soc. B* **1960**, 385.

(15) The energy of solvation (G_s) of the ions is already included in the E_{ox} and E_{red} which typically are measured in polar solvents. Differences in G_s between high dielectric solvents are negligible because $\Delta G_s \propto (1/\epsilon_1 - 1/\epsilon_2)$. The Coulombic term ($e^2/\epsilon R$) is also insignificant in polar solvents as, for example, in water where $C \simeq -2.9$ eV/$\epsilon \simeq -0.04$ eV.

(16) Interestingly, a "reverse" CT state of comparable energy is predicted at low pH with the pyrene ring as donor ($E_{ox} = 1.2$ V) and the anilinium ring as acceptor ($E_{red.} = -1.36$ V [17]). However, the susceptibility of the observed CT state to proton-transfer quenching and the pH dependence of the CT fluorescence are consistent with the state having pyrene as acceptor and aniline as donor.

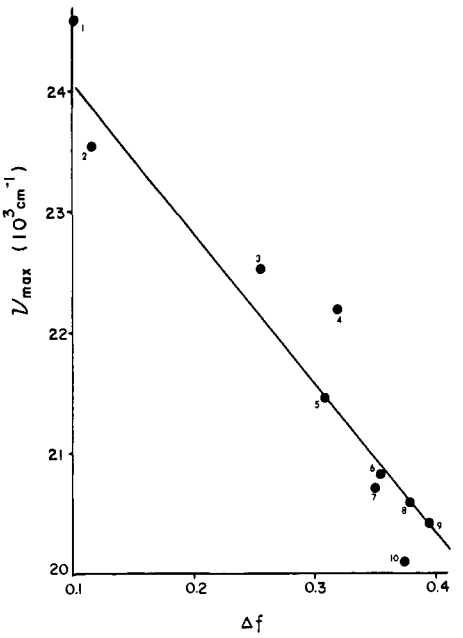

Figure 2. Plot of wavelength maxima for charge-transfer fluorescence as a function of solvent polarity as shown in eq 2 for (1) methylcyclohexane, (2) benzene, (3) diethyl ether, (4) dichloromethane, (5) tetrahydrofuran, (6) benzonitrile, (7) *n*-pentanol, (8) ethanol, (9) acetonitrile, and (10) glycerol.

composite of pyrene and aniline chromophores. Absorption in the near-UV region is dominated by the intense π,π^* transitions (E_S = 3.34 eV) of the pyrene ring (Figure 1). While the absorption spectra in alcohol–water (50:50) show rather similar band maxima at low (anilinium form) or high (free base form) pH, a tail toward the visible is noticeable in basic solution. This slight red shift is most easily understood as a *small* contribution from CT interaction in the free base which is limited by the relatively large dihedral angle between the pyrene and aniline moieties in the ground state. This interaction is not possible at low pH when I exists in the conjugate acid form.

Fluorescence Spectra. Two principal types of emission are observed from I. In most organic solvents, a single fluorescence is seen as a broad, structureless band with a spectral position very dependent on solvent polarity (Table I). This short-lived (a few nanoseconds, see below) fluorescence ranges between ~410 nm in nonpolar to ~510 nm in polar media. A different fluorescence is observed in aqueous media at sufficiently low pH that I exists in its conjugate acid form. This longer lived (~30 ns) fluorescence centered near 400 nm is structured, displays a mirror-image relationship to the absorption spectrum, and is insensitive to change in solvent polarity. On the basis of the above characteristics, the longer and shorter wavelength emissions are attributed to CT and locally excited π,π^* states, respectively.

Evaluation of Solvent Dependence of CT Fluorescence. The position of the CT fluorescence maximum in highly polar media (near 500 nm, ~2.5 eV) agrees reasonably well with the predicted value derived from the redox energetics (2.7 eV). A further indication of the highly polar nature of this state is available from the dependence of the electronic transition energy on bulk solvent dielectric constant[18]

$$\nu_{fl} = \nu_{fl}(0) - 2\mu_e^2\Delta f/hca^3 \quad (2)$$

$$\Delta f = [(\epsilon - 1)/(2\epsilon - 1)] - (n^2 - 1)/(4n^2 + 2) \quad (3)$$

where h is Planck's constant, c is the speed of light, ν_{fl} is the fluorescence maximum in a solvent of dielectric constant ϵ and refractive index n, $\nu_{fl}(0)$ is the gas-phase value of the fluorescence maximum, and μ_e is the excited-state dipole moment. The greatest uncertainty in these calculations is in a, the "effective" radius of the solvent shell around the molecule which is usually taken as 40% of the major axis for an approximately ellipsoidal solvent cavity. The slope of a plot of ν_{fl} vs. Δf (Figure 2), using a = 5.2 Å, indicates an excited-state dipole moment of 14.3 D for I. For comparison, a similar study indicates μ_e = 18 D in the TICT state of 4-(9-anthryl)-*N*,*N*-dimethylaniline.[15] These large calculated dipole moments suggest an excited state formed by complete, or nearly complete, charge transfer between the donor and acceptor groups (eq 1).

(17) Mayell, J. S.; Bard, A. J. *J. Am. Chem. Soc.* **1963**, *85*, 421.
(18) (a) Onsager, L. *J. Am. Chem. Soc.* **1936**, *58*, 1483. (b) Liptay, W. In "Modern Quantum Chemistry"; Sinanoglu, O.; Ed.; Academic Press: New York, 1966. (c) Mataga, N. in "The Exciplex"; Gordon, M., Ware, W., Eds.; Academic Press: New York, 1975.

Table II. Measured and Derived Photophysical Parameters

	short-wavelength fluorescence			long-wavelength fluorescence		
solvent	Φ_f[a]	τ_f, ns	$k_r \times 10^{-7}$, s^{-1}	Φ_f[a]	τ_f, ns	$k_r \times 10^{-7}$, s^{-1}
cyclohexane	0.36	7	5.1			
tetrahydrofuran				0.71	5	14
ethanol				0.75	7	11
acetonitrile				0.68	7	9.7
ethanol–water (50:50), pH 7				0.39	2.6 ± 0.2[b]	15
ethanol–water (50:50), 6 M HCl	0.29	57	0.51			

[a] Measured relative to quinine sulfate. [b] Using the deconvolution procedure described in the Experimental Section.

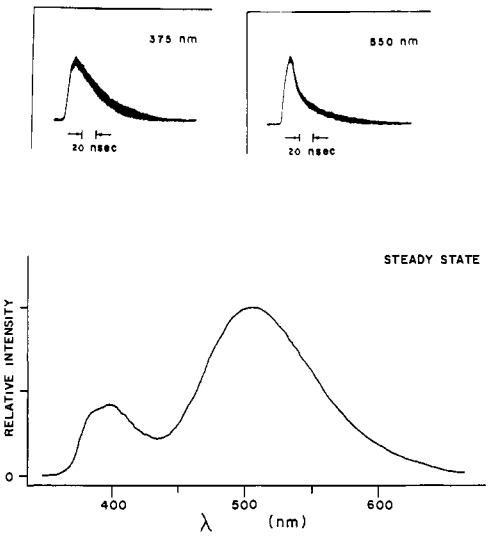

Figure 3. Fluorescence emissions from 1-(*p*-aminophenyl)pyrene in ethanol–water (50:50) at pH 4.0. Lower: Steady-state emission spectra. Upper: Fluorescence decays at 375 and 550 nm. Note the biphasic behavior of the latter.

Transient Experiments and Quantum Yield Measurements. Exponential decays were observed from I in all organic solvents and in aqueous solvents at neutral and basic pH's. The fluorescence lifetimes, quantum yields, and derived radiative rate constants appear in Table II. The short-wavelength fluorescence from I in ethanol–water under acidic conditions (pH = 1) is exponential but with rather different photophysical parameters in comparison with the long-wavelength emission. The former is longer lived with an appreciably smaller radiative rate constant in agreement with the excited-state assignments. At pH 4.0, where I is partially protonated in the ground state, both short- and long-wavlength fluorescences are observed. The former is exponential but the latter is biexponential showing fast (a few nanoseconds) and slow (lifetime identical with that of short wavelength) components (Figure 3). A series of fluorescence spectra recorded in various time periods following nitrogen laser excitation (Figure 4) shows only contributions from the π,π^* and CT emissions. The

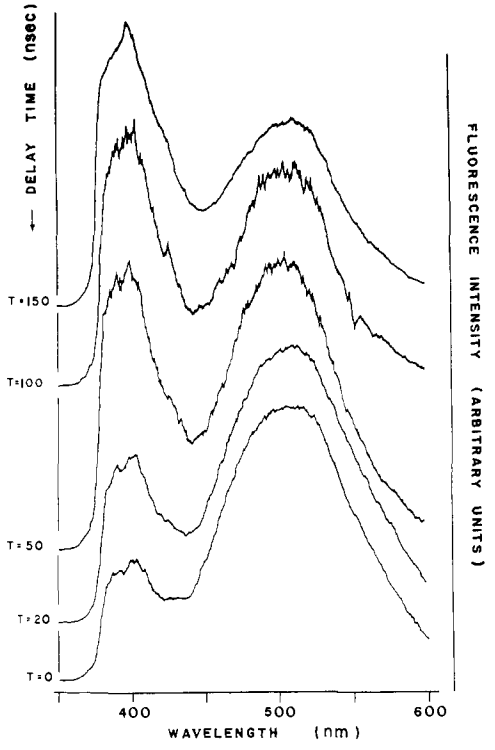

Figure 4. Time-resolved fluorescence spectra of 1-(*p*-aminophenyl)pyrene in ethanol–water (50:50) at pH 4.0 recorded with a sampling gate of 10 ns. Reported delay times should only be taken as an indication of the relative time characteristics of the emissions.

composition changes rapidly during early time (due to a faster decay of the CT emission) but then reaches a constant ratio reflecting the common lifetime of the two emissions at longer times. These results demonstrate that the CT state is populated by both direct excitation and a second channel involving deprotonation of the locally excited π,π^* state of the conjugate acid as shown in Figure 5.

Excited-State Acidity. The excited-state acidity of the conjugate acid of I was estimated by a Forster cycle[19] which relates the pK_a^* to the 0,0 transition energies of the acid/base pair and the pK_a by the relationship

$$pK_a^* = pK_a = (2.1 \times 10^{-3})\Delta\nu \quad (4)$$

where $\Delta\nu$ is the difference in transition energies in wavenumbers.[20] In cases where the 0,0 transition energies are unavailable, reasonable approximations may be obtained by use of the absorption maxima.[20] This latter approach leads to an estimate of $pK_a^* = 3.3$ in ethanol–water (50:50) and indicates only a slight enhancement in acidity in the excited state over the ground state. Note that the fluorescence titration method is not applicable to this system because of the absence of an established proteolytic equilibrium in the excited state. All available experimental data indicate that the excited free base only relaxes to the CT state so that *an equilibrium is never established* between I*-H^+ and I* (where both are locally excited π,π^* states).

The very modest difference between the pK_a^* and pK_a values deserves some further comment. More typically, aryl amines show rather large enhancements in acidity in the excited states as seen in the following examples (pK_a^*/pK_a): 1-aminonaphthalene (-1.0/3.9);[21a] 2-aminonaphthalene (-0.8/4.1);[21a] 1-aminoanthracene (-5.5/3.3);[21b] 1-aminopyrene (-5.8/2.8).[21c] In these cases the acid/base function is *directly attached* to the π-electron system that is photoexcited with the enhanced acidity arising from a strong CT contribution to the free base excited state.

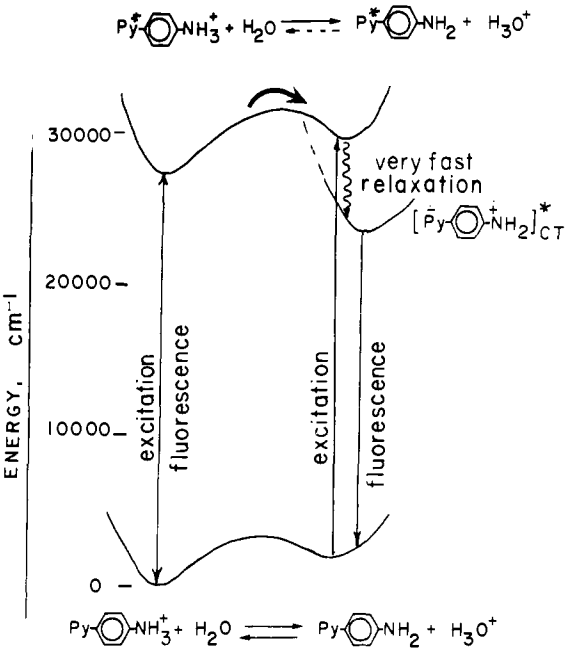

Figure 5. Photophysical scheme for 1-(*p*-aminophenyl)pyrene in ethanol–water (50:50). Estimated energies of the π,π^* and CT states are 27 400 and 22 500 cm^{-1}, respectively. The arrow denotes deprotonation of the conjugate acid form in the excited state.

The similar acidities of the ground and excited states of I indicate little or no CT contribution to the excited state during deprotonation. One interpretation is that the excitation is localized in the pyrene ring until some point after the transition state for deprotonation has been passed with subsequent relaxation into the CT state as shown in Figure 5.

Proton-Transfer Quenching of the CT State. The quantum yield of the CT fluorescence shows a pH dependence in acidic media as shown by the Stern–Volmer plot in Figure 6. Over this range of acid (0.01–1.0 M HCl), the CT state is formed exclusively by deprotonation of I*-H^+ since there is little or no measureable free base in the ground state. Proton quenching of the precursor state (I*-H^+) is not involved since the lifetime of the π,π^* fluorescence does not change over this pH range. A more likely explanation is proton transfer quenching of the CT state for which there is ample precedent.[22] Further, in the methoxynaphthalenes,[22c] H/D isotope labeling experiments have shown that quenching occurs with protonation of the ring carbons of the naphthalene ring consistent with the charge distribution in the CT state. It is reasonable to assume that the pH dependence of the CT fluorescence from I also results from this same type of proton-transfer quenching.

The plot of Figure 6 ignores the changing proton activity coefficients in this solvent system and, accordingly, does not provide a reliable estimate of k_q, the bimolecular rate constant for proton-transfer quenching by the Stern–Volmer relationship

$$\Phi_0/\Phi = 1 + k_q\tau_f[Q] \quad (5)$$

Unfortunately, pH measurements are not a direct measure of proton activities because of the residual liquid junction potential at the salt bridge of the electrodes which introduces a systematic error (which depends on the solvent system).[23] However, proton

(19) Forster, Th. *Naturwissenschaften* **1949**, *36*, 186.
(20) Ireland, J. F.; Wyatt, P. A. H. In "Advances in Physical Organic Chemistry"; Gold, V., Bethell, D., Eds.; Academic Press: New York, 1976; Vol. 12.
(21) (a) Tsutsumi, K.; Shizuka, H. *Chem. Phys. Lett.* **1977**, *52*, 485. (b) Rotkiewicz, K.; Grabowiski, Z. R. *Trans. Faraday Soc.* **1969**, *65*, 3263. (c) Shizuka, H.; Tsutsumi, K.; Takeuchi, H.; Tanaka, I. *Chem. Phys. Lett.* **1979**, *62*, 408.
(22) (a) Forster, Th. *Chem. Phys. Lett.* **1972**, *17*, 309. (b) Tsutsumi, K.; Shizuka, H. *Chem. Phys. Lett.* **1977**, *52*, 485. (c) Tobita, S.; Shizuka, H. *Chem. Phys. Lett.* **1980**, *75*, 140. (d) Harris, C.M.; Selinger, G. K. *J. Phys. Chem.* **1980**, *84*, 891. (e) Shizuka, H.; Tsutsumi, K.; Takeuchi, H.; Tanaka, I. *Chem. Phys.* **1981**, *59*, 183. (f) Shizuka, H.; Tobita, S. *J. Am. Chem. Soc.* **1982**, *104*, 6919. (g) Tsutsumi, K.; Sekigushi, S.; Shizuka, H. *J. Chem. Soc., Faraday Trans. 1* **1982**, *78*, 1087. (h) Shizuka, H.; Tsutsumi, K. *Bull. Chem. Soc. Jpn.* **1983**, *56*, 629.

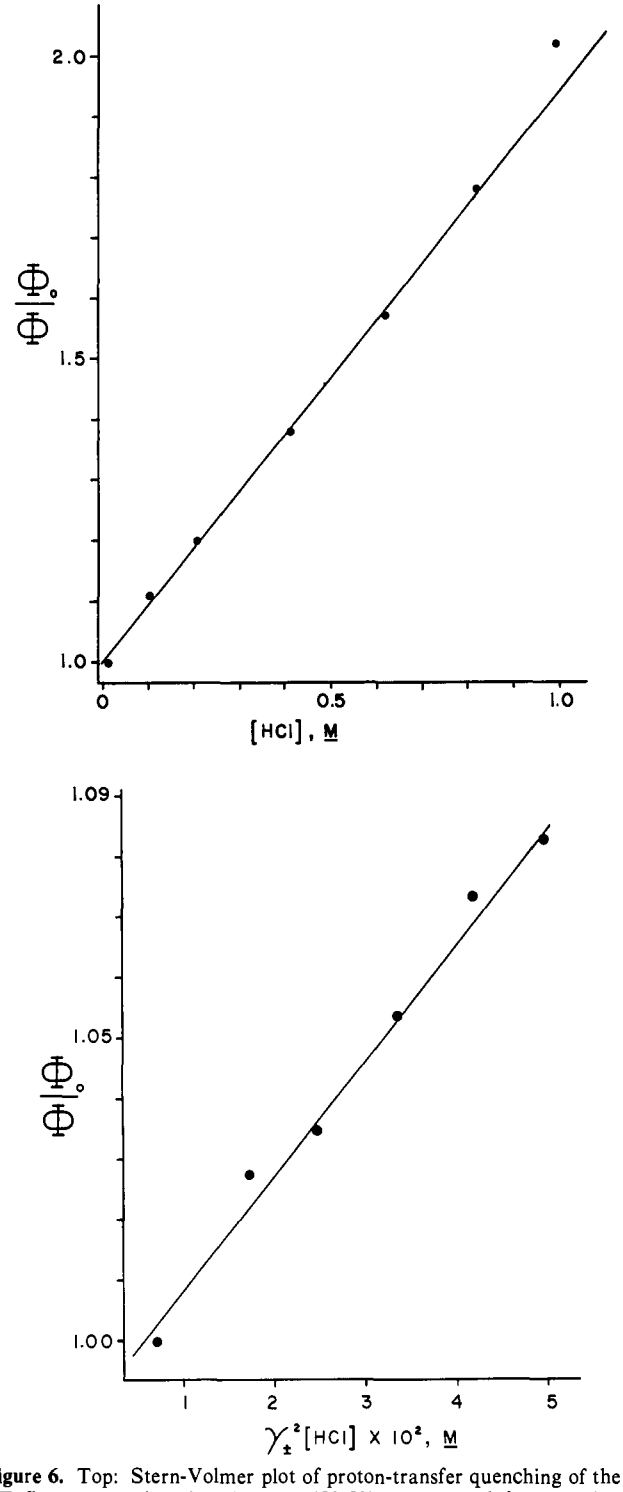

Figure 6. Top: Stern-Volmer plot of proton-transfer quenching of the CT fluorescence in ethanol–water (50:50) uncorrected for changing proton activity. Bottom: Stern–Volmer plot in the same medium corrected as described in the text.

activity coefficients have been determined by others[24] in ethanol–water (50:50) over a portion of the plot in Figure 6 (up to ~0.1 M). Although this range covers only 8% quenching of the CT fluorescence, we were able to obtain rather good results in a steady-state experiment by carefully measuring the CT emission yield relative to the unchanging π,π^* emission (Table III).

In the present experiment, electrostatic influences on the quenching step are important. Harris and Selinger[22d] recently pointed out that proton-transfer quenching shows a dependence on $[H^+](\gamma_\pm)^{-2Z}$, where $\gamma_\pm$ is the mean activity coefficient of the acid in the medium and Z is the charge of the species being quenched. On the basis of a model of complete electron transfer in the TICT state of I, proton transfer occurs to a pyrene radical anion species so that $Z = -1$. From the slope of the steady-state quenching data against $[HCl](\gamma^2)$ (Figure 6, inset), and using a fluorescence lifetime of 2.6 ± 0.2 ns, is derived $k_q = (7.38 \pm 1.5) \times 10^8$ M^{-1} s^{-1}. For comparison with other literature data, the slope of the plot in Figure 6 yields a k_q (uncorrected for proton activity coefficients) of $(3.6 \pm 0.7) \times 10^8$ M^{-1} s^{-1}. Both the corrected and uncorrected treatments indicate that proton transfer quenching of the TICT state approaches, but is clearly less than, the diffusion limit.

Table III. Data for Proton-Transfer Quenching over the pH Range 1.4–2.4 in Ethanol–Water (50:50)

			fluorescence intensities	
[HCl] × 10^{-2},[a] M	pH	$\gamma_\pm$[b]	$R = I_{LW}/I_{SW}$[c]	R_0/R[d]
1.0	2.33	0.83	0.747	(1.00)
3.1	1.93	0.75	0.727	1.02
5.2	1.77	0.70	0.722	1.03
7.3	1.62	0.69	0.709	1.05
9.4	1.52	0.68	0.696	1.07
11.4	1.44	0.68	0.690	1.08

[a] Analytical HCl concentration. [b] Mean activity coefficients for HCl in ethanol–water (50:50) as interpolated from the data in ref 24. [c] Ratio of the long-wavelength to short-wavelength fluorescence intensities. [d] R_0 is R for first line in the table so that R_0/R is equivalent to Φ_0/Φ.

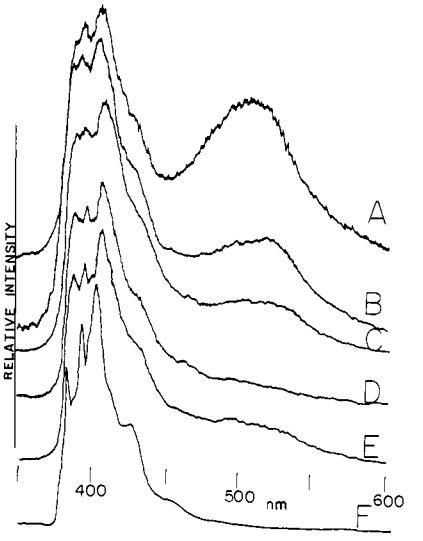

Figure 7. Time-resolved fluorescence spectra of 1-(*p*-aminophenyl)pyrene in ethanol–water (50:50) acidified with 0.1 M HCl (all with a sampling gate of 20 ns and a delay time of 0 to 20 ns). Temperatures in °C: (±1 °C): A, 19; B, −2; C, −20; D, −46; E, −63; F, −196.

Variable Low-Temperature Studies in Acidic Ethanol–Water. Time-resolved fluorescence spectra and decay curves were obtained over a wide temperature range for I in ethanol–water (50:50) acidified with 0.1 M HCl. At room temperature (22 °C), identical lifetimes of 28 ns are observed for the π,π^* and CT emissions, indicating all of the latter is derived from the former at this pH (1.4). As the temperature is lowered, the ratio of the CT/π,π^* emission yield decreases (Figure 7). At −19 °C, the CT fluorescence decay begins to display a biexponential form composed of fast (a few nanoseconds) and slow (lifetime identical with that of π,π^* fluorescence) components. The fast component is assigned to direct excitation of I (as the free base) due to a possible temperature-induced increase in ground-state acidity. Also noticeable with decreasing temperature is increasing resolution of vibrational bands in the π,π^* fluorescence. As the temperature is lowered toward the freezing point (−50 °C), the deprotonation process becomes insignificant so that most of the CT fluorescence

(23) Bates, R. G. "Determination of pH. Theory and Practice", 2nd ed.; Wiley: New York, 1973; pp 243–251.
(24) Ivanov, A. I.; Slovetskii, V. I.; Shevelev, A. A; Fainzil'berg, A. A.; Novikov, S. S. *Izv. Akad. Nauk SSR, Ser. Khim.* **1967**, 61.

Table IV. Lifetimes of Short-Wavelength π,π^* Fluorescence as a Function of Temperature in Acidic Ethanol–Water (50:50)[a]

T, °C (±0.2)	τ_f, ns	$k_{-H^+} \times 10^{-6}$,[b] s^{-1}
21.6	28.0 ± 0.4	30.3
9.9	39.7 ± 1	19.8
−0.2	52.5 ± 3	13.6
−10.3	66.2 ± 0.8	9.69
−19.1	76.5 ± 1	7.65
−28.2	88.9 ± 1	5.83
−37.1	100.8 ± 1	4.50
−47.0	108 ± 1	3.84
−53.0	105.2 ± 2	4.09
−78.9	127 ± 2	2.45
−112.6	146.2 ± 2	1.42
−142.5	167 ± 3	0.57
77 K	(184.5 ± 3)[c]	

[a] Sample contained 1.5×10^{-5} MI and was acidified with 0.1 M HCl. [b] Derived using eq 7. [c] Limiting lifetime, τ_{77}, used in eq 7.

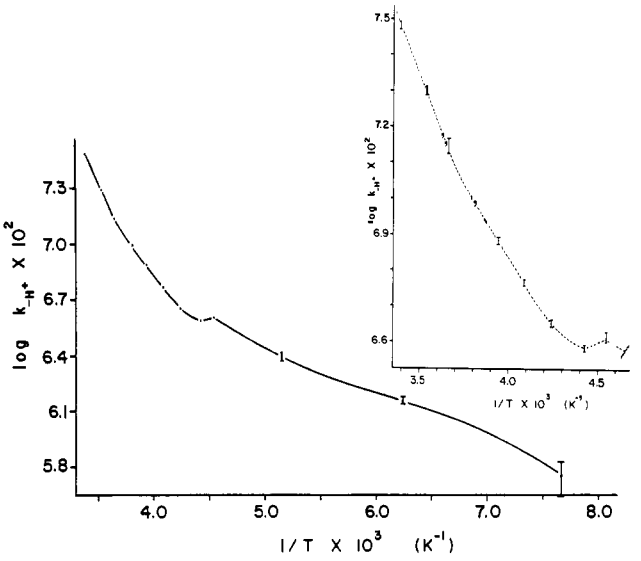

Figure 8. Arrhenius plot of excited-state proton-transfer rates in ethanol–water (50:50) at pH 1.4. Inset: An expanded view of the portion of the plot covering the liquid phase.

is of the "prompt" variety. At the phase transition, there is an increase in the relative amount of CT fluorescence which is associated with a sudden increase in the rate of deprotonation of $I^*\text{-}H^+$ (discussed below). Below the phase transition, the CT fluorescence is increasingly dominated by the prompt component. At 77 K, the π,π^* fluorescence has lengthened to 184 ns since deprotonation is negligible as indicated by the presence of only a prompt CT fluorescence.

Temperature Dependence of the Rate of Deprotonation. The change in lifetime of the π,π^* fluorescence with temperature can be used to determine the temperature dependence of the deprotonation process. If the fluorescence lifetime of $I^*\text{-}H^+$ at a given temperature is given by

$$\tau_f = (k_1 + k_{-H^+})^{-1} \quad (6)$$

where k_1 represents all first-order temperature-independent processes (including fluorescence) and k_{-H^+} is the temperature-dependent deprotonation step, and assuming that the lifetime at 77 K = $1/k_1$, then

$$k_{-H^+} = \tau_f^{-1} - \tau_{77}^{-1} \quad (7)$$

Table IV lists the lifetime data and derived values for k_{-H^+}. The Arrhenius plot in Figure 8 clearly shows two regions above and below the discontinuity in the phase transition region. The liquid region plot is enlarged in the inset. Analysis of the limiting slope in the high-temperature region of the liquid phase leads to an activation energy of 5.95 kcal/mol and a preexponential of $A = 7.8 \times 10^{11}$ s^{-1}. Noticeable curvature begins to appear in the Arrhenius plot near −10 °C, well above the region of the phase transition. A sharp increase in curvature occurs near −40 °C with a sharp discontinuity occurring at the phase transition. This unexpected increase in the rate of deprotonation is responsible for the increase in the CT fluorescence at the phase transition. Some curvature is apparent immediately below the phase transition before the onset of a limiting slope in the very low temperature range (around −110 °C) with a calculated activation energy for this region of 1.1 kcal/mol, about 20% of the value at room temperature.

Table V. Activation Parameters for Proton Transfer in Ethanol–Water (50:50)

T, K	$\Delta H^\ddagger$, cal/mol	$\Delta S^\ddagger$, cal/(K·mol)	$T\Delta S^\ddagger$, cal/mol	$\Delta G^\ddagger$, cal/mol
295	5360	−6.1	−1800	7160
250	3164	−14.3	−3562	6730
160	780	−24.3	−3888	4668

The enthalpy ($\Delta H^\ddagger$) and entropy ($\Delta S^\ddagger$) of activation for the deprotonation step in the several different temperature regions identified by the Arrhenius plot appear in Table V. At room temperature, the enthalpic term dominates and the free energy of activation (7.2 kcal/mol) is slightly larger than the free energy change (ΔG = 6.2 kcal/mol) associated with excited-state equilibrium (K_a^*). Thus, the deprotonation rate at room temperature correlates with expectations based on thermodynamic observations.

In the lower temperature regions, the trend is toward decreasing enthalpic and increasing entropic (more negative $\Delta S^\ddagger$) contributions to the kinetic barrier for proton transfer. A good example is a comparison of the values in Table V at 295 and 250 K. Striking differences are noted in the $\Delta H^\ddagger$ and $\Delta S^\ddagger$ values even though both are derived from liquid-phase reactions only 45 K apart. Below, the phase transition, even more dramatic differences are noted.

Nonlinear Arrhenius plots of proton-transfer reactions have been known for many years[25] with explanations ranging from quantum-mechanical[26] to quasithermodynamical[25] effects. More recently, such behavior in binary aqueous solutions has been explained in terms of a pseudo-phase-separation model.[27] Although a unique explanation cannot be offered for the above photophysical observations in alcohol–water, this study does point out the versatility of I as a probe of proton-transfer reactions. We will separately report our results of a study with I in cationic and anionic micelles.

Conclusions. This study demonstrates that chemical (proton transfer) and electronic ($\pi,\pi^* \rightarrow$ TICT state) photophysical processes may be uncoupled through proper design of the system. Our results with I suggest that the locally excited π,π^* free base state is a short-lived intermediate in the excited-state deprotonation scheme possibly accessible by subnanosecond laser techniques. In this way, experiments may be directed toward identifying key factors involved in the development of the CT state. The close to diffusion-controlled rate of proton-transfer quenching of the TICT state is consistent with a species having properties of its radical ion components. Such chemical trapping experiments may be exploited in designing solar energy conversion and storage systems. Finally, the pH influences on the formation and destruction of the TICT state of I are important for the photosynthetic, charge-separated,[28] and bichromophoric[29] systems which

(25) (a) Hulett, J. R. *Q. Rev. Chem. Soc.* **1964**, 18, 227 and references therein. (b) Bell, R. P. "The Proton in Chemistry", 2nd ed.; Cornell University Press: New York, 1973; pp 270–289.

(26) For a more recent example see: Peters, K.; Applebury, M. L.; Rentzepis, P. M. *Proc. Natl. Acad. Sci. U.S.A.* **1977**, *74*, 3119.

(27) Holterman, H. A. J.; Engberts, J. B. F. N. *J. Org. Chem.* **1983**, *48*, 4025 and references therein.

(28) (a) Lindsey, J. S.; Mauzerall, D. C.; Linschitz, H. *J. Am. Chem. Soc.* **1983**, *105*, 6528. (b) McIntosh, A. R.; Siemiarczak, A.; Bolton, J. R.; Stillman, M. J.; Ho, T.-F.; Weedon, A. C. *J. Am. Chem. Soc.* **1983**, *105*, 7215. (c) Siemiarczak, A.; McIntosh, A. R.; Ho, J.-H.; Stillman, M. J.; Roach, K. J.; Weedon, A. C.; Bolton, J. R.; Connolly, J. S. *J. Am. Chem. Soc.* **1983**, *105*, 7224.

are currently of great interest.

Experimental Section

Synthesis of I. Isomeric 1- and 2-(*p*-Nitrophenyl)pyrenes. To a cooled solution (5 °C) of *p*-nitroaniline (8.4 g, 64 mmol) in 300 mL of water and 10 mL of concentrated hydrochloric acid was added a 60 mL of an aqueous solution of sodium nitrite (4.6 g, 68 mmol) all at once. The resulting solution of the diazonium salt was added, under a nitrogen atmosphere, to a solution of pyrene (6.5 g, 32 mmol) in acetone saturated with sodium acetate. The reaction mixture was stirred at room temperature overnight, and the deposited solid was filtered off. The liquid phase was concentrated in vacuo, and the resulting residue was washed with ether. The dried ether washings were combined with the previously recovered solid and evaporated. The resulting material was chromatographed on neutral alumina with gradient elution (petroleum ether/dichloromethane). After some unreacted pyrene was recovered, a yellow solid was eluted first (2.24 g, 22%, mp 114–117 °C) followed by an orange solid (0.67 g, 6.5%, mp 268–270 °C). Mass spectral analyses of the two products on a Hewlett-Packard 5985A GC mass spectrometer provided results consistent with the desired products. Yellow product, nominal mass: 323.3 (th. 323.37); relative intensities. M/M + 1/M + 2, 100/23.4/3.05 (th. 100/24.4/3.2). Orange product, nominal mass: 323.4 (th. 323.37); relative intensities: M/M + 1/M + 2, 100/23.7/3.2 (th. 100/24.4/3.2). The assignments of the 1- and 2-positional isomers to the yellow and orange products, respectively, were based on NMR analyses of the corresponding anilines.

Isomeric 1- and 2-(*p*-Aminophenyl)pyrenes. To 1-(*p*-nitrophenyl)-pyrene (the yellow isomer) (1.5 g, 4.6 mmol) in 250 mL of ethanol–water (4:1) were added an excess of tin metal (5 g) and 15 mL of concentrated hydrochloric acid. The mixture was refluxed, and more acid was periodically added. After 1 h, the reaction mixture was cooled and the precipitated salts and residue from the evaporated solution were washed with water followed by dichloromethane and then air dried. The product was recovered as the hydrochloride salt: pale yellow crystals (1.2 g 82%).

2-(*p*-Nitrophenyl)pyrene was reduced in a similar manner except that a longer reaction time was required. A partially dissolved suspension of the orange isomer in ethanol–water (3:1) was refluxed with Sn/HCl under a nitrogen atmosphere for 6 h. During the course of the reaction, a yellow product precipitated. At the end of the reaction, it was collected by suction filtration, washed with water and ethanol, and air dried.

The hydrochloride salts were converted to the free bases as follows. Powdered crystals of the salt of 1-(*p*-aminophenyl)pyrene (110 mg) were added to 30 mL of dichloromethane (reagent grade) in a 60-mL separatory funnel followed by 20 mL of 20% aqueous sodium hydroxide. The mixture was shaken for 10–15 min until most of the solid had dissolved. The dichloromethane solution was separated, extracted one more time with 20 mL of aqueous sodium hydroxide, drawn off through a plug of glass wool in the stem of the separatory funnel, and dried over sodium sulfate. The solution was evaporated to an oil which slowly crystallized. The product was redissolved in 1 mL of dichloromethane with warming. Upon cooling, light green needles formed which were recovered by suction filtration and stored in the dark. (40 mp 181–3 °C). Mass spectra: nominal mass, 293.3 (th. 293.37); relative intenstiies: M/M + 1/M + 2, 100/25.5/2.8 (th. 100/24.6/2.9). Similar treatment of the hydrochloride of the 2-isomer yielded a greenish-yellow solid. Fourier transform NMR spectra of the free base forms of the 1-and 2-isomers were recorded on a Varian XL-100-15 spectrometer. The 1- and 2-isomers were distinguished by their respective FT ^{13}C spectra. Because of the higher symmetry of the 2-isomer, there are only 14 magnetically distinct carbon nuclei compared with 20 in the 1-isomer. In the broad-band decoupled ^{13}C NMR spectrum of the latter, over 16 distinct resonances are observed.

Physical Measurements. Materials. Solvents used were either spectroquality or reagent grade. Acetonitrile was purified by drying over phosphorus pentoxide and distilling from calcium hydride. Commercial distilled water was redistilled two times from alkaline potassium permanganate. Pyrene (Aldrich) was chromatographed on alumina and sublimed prior to use.

Cyclic Voltammetry. Measurements were conducted at ambient temperature (~22 °C) on a quiet soluton that had been purged with nitrogen gas for 15 min in a standard three-electrode CV cell, using a Bioanalytical Systems (BAS) model CV-1B apparatus. The reference electrode was Ag/AgCl, the counterelectrode was a platinum wire which had been cleaned by dipping in nitric acid, and two types of working electrodes were used. For scans at positive potentials (relative to NHE), a vitreous carbon electrode which had been polished with polishing alumina was used. For scans at negative potentials, a mercury/gold amalgam electrode was used. Voltammograms were recorded on a Houston Instrument Omnigraphic 2000 X–Y recorder. Measurements on I (2×10^{-4} *M*, pH 7) were carried out in ethanol–water (55:45) containing tetra-*n*-butylammonium perchlorate (TBAP)[30] (0.1 M) as supporting electrolyte. Measurements on pyrene (~10^{-4} M) in ethanol–water (65:35) were carried out under similar conditions.

Spectroscopic Measurements. Ultraviolet–visible absorption spectra were recorded on a Beckman Acta M VI spectrophotometer. Steady-state emission spectra were recorded on an American Instrumen Co. spectrofluorimeter with a Hamamatsu R446 photomultiplier tube. Spectra were not corrected for instrument throughput and response. Time-resolved emission spectra were recorded on a pulsed nitrogen laser (337 nm, 10 ns, peak power 100 kW) in conjunction with a Princeton Applied Research boxcar integrator (Model 160) as previously described.[31] Fluorescence decays were measured as follows. The signal from the photomultiplier was directly inputted into a Hewlett-Packard 183A oscilloscope (50 Ω termination) and photographically recorded. The original tracing was photographically enlarged and analyzed. Where necessary, the method of iterative convolutions[32] was used for deconvolution of the experimental fluorescence decay. A Fortran IV program was written to perform the iterative convolution procedure on monoexponential as well as biexponential decay functions. Recursion formulas based on the convolution integral for the fitting function, and its partial derivative with respect to the parameters being varied, were taken from the literature[33] as were the routines for fitting of parameters and minimization of error by the nonlinear least-squares procedure.[34]

Acknowledgment. We thank Mr. Mark Gorwitz for preparation of the title compound and Prof. C. Francis for use of his CV apparatus.

Registry No. I, 87393-65-5; 1-(*p*-nitrophenyl)pyrene, 95069-74-2; 2-(*p*-nitrophenyl)pyrene, 95069-75-3; *p*-nitroaniline, 100-01-6; pyrene, 129-00-0; 1-(*p*-aminophenyl)pyrene hydrochloride, 95069-76-4; 2-(*p*-aminophenyl)pyrene hydrochloride, 95069-77-5; 2-(*p*-aminophenyl)pyrene, 95069-78-6.

(29) (a) Calcaterra, L. T.; Closs, G. L.; Miller, J. R. *J. Am. Chem. Soc.* **1983**, *105*, 670. (b) Miller, J. R.; Calcaterra, L. T.; Closs, G. L. *J. Am. Chem. Soc.* **1984**, *106*, 3074. (c) Mes, G. F.; de Jong, B.; Van Ramesdonk, H. J.; Verhoeven, J. W.; Warman, J. M.; de Haas, M. P.; Horsman-van den Dool, L. E. W. *J. Am. Chem. Soc.* **1984**, *106*, 6524 and references therein.

(30) Makosza, M.; Bialecka, E. *Synth. Commun.* **1976**, *6*, 313.

(31) Brown, R. E.; Legg, K.; Wolf, M. W.; Singer, L. A.; Parks, J. H. *Anal. Chem.* **1974**, *46*, 1690.

(32) McKinnon, A. E.; Szabo, A. G.; Miller, D. R. *J. Phys. Chem.* **1977**, *81*, 1564.

(33) Grinvald, A.; Steinberg, I. Z. *Anal. Biochem.* **1974**, *59*, 583.

(34) Bevington, P. V. "Data Reduction for the Physical Sciences"; McGraw-Hill: New York, 1969.